

# GraphIFE: Rethinking Graph Imbalance Node Classification via Invariant Learning

Fanlong Zeng, Wensheng Gan\*, Philip S. Yu, *Life Fellow, IEEE*

**Abstract**—The class imbalance problem refers to the disproportionate distribution of samples across different classes within a dataset, where the minority classes are significantly underrepresented. This issue is also prevalent in graph-structured data. Most graph neural networks (GNNs) implicitly assume a balanced class distribution and therefore often fail to account for the challenges introduced by class imbalance, which can lead to biased learning and degraded performance on minority classes. We identify a quality inconsistency problem in synthesized nodes, which leads to suboptimal performance under graph imbalance conditions. To mitigate this issue, we propose GraphIFE (Graph Invariant Feature Extraction), a novel framework designed to mitigate quality inconsistency in synthesized nodes. Our approach incorporates two key concepts from graph invariant learning and introduces strategies to strengthen the embedding space representation, thereby enhancing the model's ability to identify invariant features. Extensive experiments demonstrate the framework's efficiency and robust generalization, as GraphIFE consistently outperforms various baselines across multiple datasets. The code is publicly available at <https://github.com/flzeng1/GraphIFE>.

**Index Terms**—Graph, imbalance learning, node classification, invariant learning, data augmentation



## 1 INTRODUCTION

Node classification is a fundamental task in the graph domain [1], [2]. Graphs are widely used to model complex relational structures among entities, where nodes typically represent individual entities (such as individuals, objects, organizations, or events) and edges denote the relationships between them. For example, a social network can be modeled as a graph in which each node corresponds to a user, and the edges capture interactions or relationships among users. Node classification has a wide range of practical applications [3], [4]. In social networks, it can be used to detect malicious users [5], [6], [7], while in protein-protein interaction networks, it facilitates the prediction of protein functions or annotations [8]. Graph neural networks (GNNs) have emerged as a powerful tool to address node classification tasks and have shown strong performance in diverse graph-related applications [9], [10]. However, most existing GNN approaches assume class-balanced distributions and therefore fail to adequately address the critical challenge of class imbalance in real-world graph-structured data [11], [12], [13]. Class imbalance occurs when the quantity of samples varies significantly between classes, leading to biased learning and degraded performance, particularly for the minority class [13]. In real-world applications, graph-structured data frequently demonstrates significant class imbalance, where minority classes are substantially underrepresented relative to majority classes [14], [15]. A representative example emerges in Netflix's user-item interaction

graph, where the node distribution exhibits pronounced structural imbalance: the cardinality of user nodes significantly exceeds video nodes by orders of magnitude. When applied to class-imbalanced graphs, conventional GNNs exhibit a systematic tendency to underrepresent minority classes, leading to biased representations and degraded generalization performance on underrepresented nodes [16]. This limitation underscores the critical need for specialized techniques that explicitly address class imbalance in graph-based learning [13], ensuring robust and equitable model performance across all classes.

Currently, research on graph imbalance has proposed many methods. These methods can be roughly categorized into two distinct types, which are node synthesis methods [17], [18], [19] and loss-modified methods [20], [21], [22]. Node synthesis methods aim to address class imbalance by augmenting the training data through the generation of synthetic nodes that belong to the minority classes. In contrast, loss-modification strategies address class imbalance by adaptively reweighting the loss function to prioritize the minority class during training, thereby correcting the training bias inherent in imbalanced datasets while preserving the original data distribution. In this paper, node synthesis is the focus of our research. After reviewing the entire process of node synthesis, we have found that the synthesized nodes exhibit the quality inconsistency problem. The problem means that the feature of the synthesized nodes may raise a potential Out-Of-Distribution (OOD) issue. Based on the results of our experiment, we discovered that the problem would lead to the performance degradation of the model for minority classification.

The primary challenge of addressing the quality inconsistency problem lies in mitigating the feature OOD of synthesized nodes. Although the objective is clear, resolving this issue remains formidable. Current methodologies lack an effective mechanism to ensure that the synthesized

- This research was supported in part by the National Natural Science Foundation of China (No. 62272196), Guangzhou Basic and Applied Basic Research Foundation (No. 2024A0419971)
- Fanlong Zeng and Wensheng Gan are with the School of Intelligent Systems Science and Engineering, Jinan University, Zhuhai 519070, China. (E-mail: flzeng1@stu.jnu.edu.cn, wsgan001@gmail.com)
- Philip S. Yu is with the University of Illinois Chicago, Chicago, USA. (E-mail: psyu@uic.edu)
- Corresponding author: Wensheng Gan

nodes maintain fidelity to the original data distribution. Moreover, existing approaches struggle to precisely detect which synthesized nodes exhibit distributional divergence. The quality inconsistency problem in synthesized nodes manifests itself primarily in the following. The features of synthesized nodes exhibit a statistically distributed bias relative to the original training set. This bias propagates through the learning process as synthesized nodes dominate the minority class training, ultimately resulting in systematically distorted feature representations and degraded generalization performance for minority-class prediction. These challenges necessitate the development of robust methodological frameworks to effectively address them.

To address the challenge, we propose GraphIFE for (Graph Invariant Feature Extraction), a framework designed to mitigate the quality inconsistency of the synthesized nodes. GraphIFE strategically circumvents the need to directly assess whether each synthesized node aligns with the original data distribution. It integrates concepts from invariant learning and the generative adversarial network (GAN) [23] to directly extract the invariant node features while employing an adversarial attacker to enhance the model’s ability to distinguish minority classes. We adopt two key concepts from graph invariant learning [24]: 1) Invariant features, which remain stable across different domains or structures and preserve predictive semantics under varying conditions. 2) Environment features, which vary across domains or graph structures but are not causally related to the prediction target. GraphIFE leverages both types of features to address these challenges. It introduces a representation alignment strategy that encourages semantically and topologically similar nodes to be close in the embedding space. Additionally, it proposes a gated mixing mechanism to support an aggressive learning strategy while simultaneously preventing noise from dominating the training process. We evaluate the effectiveness of our proposed method across a diverse range of benchmark datasets, including citation networks (Cora, Citeseer, and PubMed) [25] and Amazon co-purchase networks (Amazon-Computers, Amazon-Photo, and Coauthor-CS) [14]. These datasets are adapted to long-tailed and imbalanced settings, following GraphENS [18] and GraphSHA [17] to better simulate real-world scenarios. Furthermore, we assess the generalizability of our approach across multiple GNN backbones, including GraphSAGE [26], GCN [27], and GAT [28]. We also conduct experiments under different hyperparameter configurations to analyze their impact on model performance. In summary, the key contributions are as follows:

- We identified that the quality inconsistency issue in the node synthesis methods, where the features of synthesized nodes may exhibit a potential OOD behavior, leading to suboptimal performance.
- We revisit the graph imbalance problem through the lens of invariant learning and propose GraphIFE, a GAN-like framework that incorporates the principles of invariant learning. GraphIFE extracts the invariant node features and employs an attacker to enhance the model’s ability to distinguish minority classes, effectively mitigating.
- Through extensive experiments, we demonstrate that

GraphIFE not only effectively mitigates the quality inconsistency issue but also achieves excellent performance across various datasets. It consistently outperforms baseline models, showcasing robust and stable results.

Following the introduction, a brief review of related work on the graph imbalance problem and graph invariant learning is provided in Section 2. The details of the quality inconsistency issue are analyzed in Section 3. Then, the preliminaries of this paper are provided in Section 4, including the comprehensive notation, the concise introduction of the node classification task, and the problem definition. The detailed implementation of GraphIFE is introduced in Section 5. The architecture and proposed mechanism are also introduced in this section. In Section 6, we present a comprehensive experimental evaluation to assess the effectiveness of GraphIFE. In addition to performance benchmarking, we conduct an in-depth analysis that includes ablation studies, visualizations, and an investigation of the sensitivity of GraphIFE to key hyperparameters. Additionally, we evaluate the performance of GraphIFE in large-scale graphs. Finally, we present our conclusions and outline future research work in Section 7.

## 2 RELATED WORK

In this section, we provide a concise review of relevant prior work, including graph imbalance methods and graph invariant learning methods.

### 2.1 Graph Imbalance Problem

The class imbalance problem represents a pervasive challenge in real-world datasets, particularly in domains requiring complex pattern recognition, such as protein-molecule interaction studies [29], [30]. This issue arises when the quantity of different classes exhibits a significantly uneven distribution, often leading models to bias predictions toward the majority class while underrepresenting the minority class [18], [22]. Such an imbalance can substantially degrade model performance, particularly in classification tasks [22]. While the class imbalance problem in graph-structured data shares similarities with its counterpart in conventional data settings, it also introduces unique complexities. In addition to disparities in class quantity, the graph class imbalance problem is characterized by topological imbalances, i.e., differences in structural connectivity between classes [18], [22]. In graph-based learning, two major approaches have been developed to address this issue: node synthesis and loss modification [20], [21], [22].

Node synthesis methods aim to mitigate class imbalance by generating synthetic nodes for minority classes, thus addressing the uneven quantity issue. For example, GraphSMOTE [11] synthesizes new minority nodes by interpolating features of two existing nodes from the same class, followed by an edge prediction step to preserve graph connectivity. GraphENS [18] constructs synthetic nodes by merging the ego-network of a minority node with that of a randomly selected node. GraphSHA [17] introduces a more discriminative approach by generating nodes from hard-to-classify samples. Methods such as ImGAGN [31]

and DR-GCN [32] apply Generative Adversarial Networks (GANs) [33] to create synthetic nodes. However, many of these methods inadequately capture the intricate topological structures inherent in real graphs. In particular, synthesizing nodes from topologically ambiguous regions can hinder model performance, as the message-passing mechanisms in GNNs tend to propagate and amplify such noise. In contrast, loss modification methods adjust the training objective to compensate for class or topological imbalances. For instance, TAM [22] introduces class-specific weights based on the distribution of node labels, while ReNode [20] adaptively modulates the contribution of each node by considering its proximity to class boundaries in the graph topology. Additionally, other recent approaches leverage contrastive learning frameworks [34], [35] or mathematical modeling techniques [36], [37] to tackle the graph class imbalance problem from alternative perspectives.

However, the above methods ignore the quality inconsistency of synthesized nodes during model training. The quality inconsistency of the synthesized node would result in a suboptimal performance of the model. GraphIFE leverages the concept of invariant learning to mitigate the adverse effects of the quality inconsistency issue.

## 2.2 Graph Invariant Learning

Invariant learning methods aim to uncover stable and domain-invariant relationships between input features and target variables. The purpose of invariant learning is to solve the problem of out-of-distribution (OOD). The OOD problem arises when the testing data distribution differs from, and is unknown relative to, the training distribution. Various strategies have been proposed to address OOD generalization [38], [39], [40]. Among them, causal inference methods seek to learn underlying variables within a causal graph in either an unsupervised or semi-supervised manner [41], [42]. By leveraging these learned causal representations, models can better capture the latent data-generating mechanisms. Graph OOD generalization poses greater complexity compared to its counterparts in other domains, as distributional shifts in graph data can manifest in diverse forms, including changes in node attributes, edge structures, or overall topology. These variations significantly complicate the identification and extraction of invariant features. The quality inconsistency of the mix node found in this paper is also a graph OOD problem. The inconsistent quality of synthesized nodes is mainly manifested in the inconsistent features of synthesized nodes with the original dataset.

Currently, two primary categories of graph-related tasks are node-level and graph-level. They are typically addressed using distinct approaches. Node-level tasks focus on predicting labels for individual nodes, which are inherently non-independent and identically distributed (non-i.i.d.) due to the interconnected nature of graph structures. In contrast, graph-level tasks consider each entire graph as a single instance and often assume that these graph instances are i.i.d., despite potential underlying correlations across graphs. This article mainly discusses the node-level graph OOD problem. Many methods to deal with node-level OOD have been proposed. SRGNN [43] employs multiple context generators

to construct diverse virtual environments and maximizes the variance of empirical risks across them. This encourages the model to explore a broader range of feature-context relationships, thereby enhancing its ability to extrapolate beyond the single observed training environment. EERM [44] is designed to address distributional discrepancies between biased training data and the true underlying inference distribution of the graph. FLOOD [41] integrates invariant representation learning with bootstrapped representation learning to enhance OOD generalization. The proposed approach seeks to strike a balance between maintaining stable representations across diverse training environments and preserving adaptability to potentially unknown test distributions. CIA-LRA [42] utilizes the distribution of neighboring labels to selectively align node representations. This approach enables the model to effectively identify and retain invariant features while filtering out spurious correlations, without requiring explicit environment labels.

However, existing methods remain limited in addressing graph imbalance scenarios. GraphIFE especially considers the graph imbalance node classification problem. It also considers the topology imbalance, selecting appropriate neighbors for the synthesized node, and extracts the essential features of the original nodes and synthesized nodes for training to mitigate the problem of graph imbalance.

## 3 QUALITY INCONSISTENCY PROBLEM

In this section, we formally characterize the quality inconsistency problem in graph imbalance scenarios and provide a theoretical analysis of it.

### 3.1 Rethinking Node Mixup

To address the node classification problem in graphs with class imbalance, a crucial step is to balance the quantity of nodes across different classes. One classic method for balancing node quantities is node mixup, which synthesizes new nodes by combining existing nodes from the minority class, thereby achieving a more balanced distribution across all classes. In recent years, a variety of node mixup methods have been proposed, including GraphENS [18], GraphSMOTE [11], and BAT [36], among others. These methods employ diverse techniques to synthesize new nodes for the minority class, aiming to balance the graph and improve classification performance in imbalanced scenarios. Nevertheless, although these methods employ metrics to evaluate the rationality of synthesized nodes—such as using KL divergence to measure the distance between synthesized nodes and original minority nodes—the quality of the synthesized minority nodes produced by these methods remains inconsistent. This raises the question of how to mitigate the impact of such inconsistent quality. The quality inconsistency issue primarily manifests as a feature distribution divergence between synthesized and original nodes.

**Feature inconsistency.** We conduct an experiment to evaluate the quality of synthesized nodes on model performance by assessing the classification performance of recent representative node mixup methods, comparing the minority class to the entire class. The intuition of the experiment is

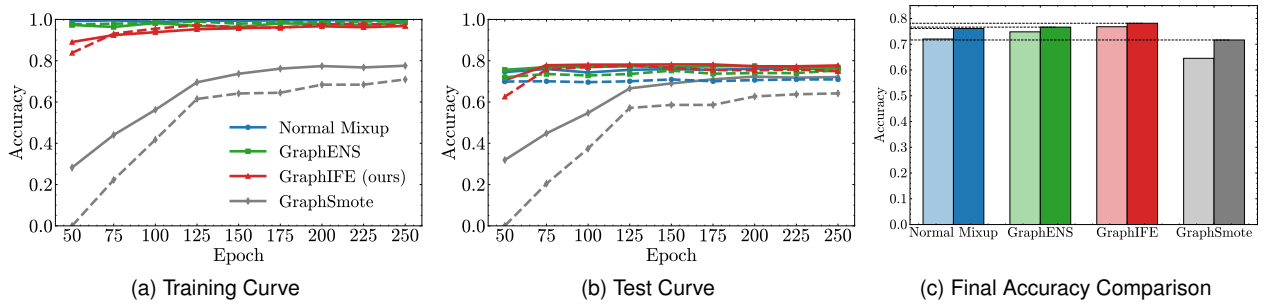


Fig. 1. The result of the training curve, test curve, and final accuracy between different node mixup methods. In the illustrated Fig. 1a and Fig. 1b, solid lines denote the learning curve of all classes and dashed lines denote the learning curve of minority classes. In illustrated Fig. 1c, dark colors represent the test accuracy of all classes, while light colors represent the test accuracy of minority classes. Notice that normal mixup only utilizes the Beta distribution to determine the mix ratio between the sampling minor node and its corresponding node. Additionally, we select the final accuracy based on the validation accuracy.

that low-quality synthesized nodes will confuse the model, leading to poor classification performance on the minority class. In our experiment, we use GCN as the GNN backbone, set the imbalance ratio to 100, and train each model for 250 epochs on the Cora dataset to obtain the results. We follow the Long-Tailed setting proposed by [18] in our Cora experiments.

As shown in Fig. 1, the training curve, test curve, and final accuracy (determined by validation accuracy) are presented. As observed in Fig. 1a and Fig. 1b, solid lines represent the learning curves for all classes, while dashed lines represent the learning curves for minority classes. The “normal mixup” approach synthesizes new nodes by mixing features in a predetermined proportion, utilizing the Beta distribution solely to determine the mix ratio between the sampled minority node and its corresponding node. As shown in the training curve Fig. 1a, a notable disparity exists between the minority node classification accuracy of GraphSMOTE and its corresponding overall class classification accuracy. This suggests that the synthesized minority nodes are not of sufficient quality to enable the model to classify the minority class effectively. In contrast, the minority node classification accuracy and overall class accuracy of other models are relatively consistent. Specifically, GraphENS, normal mixup, and GraphIFE exhibit similar gaps between their minority node and overall class accuracy. As shown in the test curve Fig. 1b, GraphIFE achieves the best performance, whereas the other methods fail to maintain their promising results from the training curve. This suggests that these mix-up methods lack good generalization capabilities. Notably, both GraphENS and GraphIFE exhibit a small gap between their minority class and overall class test curves, with GraphIFE performing slightly better. In the accuracy comparison Fig. 1c, dark colors denote the test accuracy for all classes, whereas light colors represent the test accuracy for minority classes. A notable observation is that the classification accuracy of minority nodes for normal mixup and GraphSMOTE exhibits a significant gap compared to the whole class accuracy. In contrast, the gap is smaller for GraphIFE and GraphENS. This suggests that the inconsistent quality of synthesized nodes has hindered the model’s ability to effectively classify the minority class. Although GraphIFE also exhibits a gap between the minor class and whole class accuracy, it has successfully narrowed

the accuracy gap between minor nodes and the whole class, ultimately achieving the top minor class classification results in this experiment.

In summary, existing node mixup methods often struggle to synthesize minority nodes of uniform quality for model training. Despite efforts to ensure consistency, the uneven quality of these nodes can create a significant gap in the model’s ability to classify minority and majority classes.

### 3.2 Theoretical Analysis

The quality inconsistency problem primarily arises from the inconsistent features of synthesized nodes. This affects node representations, confusing the GNN during training and leading to performance degradation. The issue is especially pronounced for the minority class, causing GNN to perform poorly in imbalanced node classification. A theoretical analysis of these aspects is provided in the following section.

Initially, we defined the notation in this analysis. Given a training dataset,  $\mathcal{D}_{tr} = \{X_{c_1}, \dots, X_{c_n}\}$ ,  $X_{c_i}$  denotes the feature set of the  $c_i$  class. In the imbalance situation, the training set can be simply divided into  $\mathcal{D}_{tr} = \{X_{min}, X_{maj}\}$ , which means the training set is composed of the feature set of the minority class and the feature set of the majority class. The label set can be divided into  $\mathcal{Y} = \{c_{1, \dots}, c_n\} = \{c_{min}, c_{maj}\}$  in the same way. Additionally, the letter with an overline above denotes the feature of a synthesized node, such as  $\bar{x}$  denotes the feature of a synthesized node. The quality inconsistency issue is especially affecting the minority class. This is due to the quantity of the synthesized minority nodes being far more than the original minority nodes. To analyze the issue (1), we have the definition:

**Definition 1.** The **feature inconsistency** issue of synthesized nodes would confuse the GNN model, making the performance of the model unable to distinguish the minority class. Its mathematical expression is as follows:

$$FI(P_{X_{syn}}, P_{X_{ori}}) = \frac{1}{2} \int_S |P_{X_{syn}}(k) - P_{X_{ori}}(k)| dk, \quad (1)$$

where  $S = \{k \in X' | \mathcal{Y}_k \in c_{min}, X' = \{X_{syn} \cup X_{ori}\}\}$ , which is the feature of the minority class after node mixup.  $P$  is a distribution.  $FI(\cdot, \cdot)$  is always mathematically bounded within  $[0, 1]$ . The formulation above means that for the minority class, the feature distribution

of the synthesized nodes is potentially different from the original training set.

The features of the synthesized node have a significant impact on the representation of the minority class and can dominate the training process. The goal of the imbalanced node classification is to balance an imbalanced dataset. Initially, the quantitative parity are ensured to be equal by node mixup. To the majority class, it has  $|X_{maj}| \gg |\bar{X}_{maj}|$ . On the contrary, to the minority class, it has  $|X_{min}| \ll |\bar{X}_{min}|$ . The letter with an overline above means it belongs to the synthesized node. In the node mixup process, there is always a mixup method to synthesize nodes. To a synthesized node  $\bar{v}$ , the feature of  $\bar{v}$  is synthesized as:

$$\begin{aligned}\bar{x} &= \text{MIXUP}(x_{sample}, x_{target}) \\ &= px_{sample} + (1-p)x_{target}.\end{aligned}$$

$p$  is the mix ratio of the different node mix-up methods. The above equation means that in the node mixup method, there always exists a different ratio to determine the mix proportion of the candidate nodes. The question that exists in this process is whether the synthesized feature would be out of distribution potentially, and without a stable quality. Additionally, due to  $|X_{min}| \ll |\bar{X}_{min}|$ , the whole training process of the minority class would dominate by the synthesized node. Without the stable feature quality, the model's performance for the minority class would be affected. The feature quality inconsistency problem can be formally represented through the following mathematical process:

*Proof:* The inconsistency issue of the node feature. After applying class balancing techniques, the resulting balanced dataset exhibits the following characteristics:  $|X'_{maj}| = |X'_{min}| \Rightarrow |X_{maj} \cup \bar{X}_{maj}| = |X_{min} \cup \bar{X}_{min}|$ . To the majority class,  $|X_{maj}| \gg |\bar{X}_{maj}|$ , the training process is dominated by the original feature. To the minority class,  $|X_{min}| \ll |\bar{X}_{min}|$ , the training process is dominated by the synthesized feature. Because,  $\bar{x} = px_{sample} + (1-p)x_{target}$ , result in  $\bar{x} \neq x$ .

To the GNN model:  $\hat{f}_\theta = \text{argmin}_{(v, c_{min}) \sim \mathcal{D}'_{tr}} [\mathcal{L}(\hat{f}_\theta(v)), c_{min}]$ .

Among others, assuming  $a = \frac{|X_{ori}|}{|X_{syn}| + |X_{ori}|}$ ,  $\hat{f}_\theta = \text{Proj}(h_v^{(l)}, h_{\bar{v}}^{(l)})$  means the representation of node  $v$  at level  $l$ .

Ignore the number of layers,  $\phi$  denotes AGG, to the representation of the minority node  $v$  in the balanced dataset:

$$\begin{aligned}h_v &= a\phi\left[\frac{1}{|u|} \sum_{u \in \mathcal{N}(v)} h_u, h_v\right] + (1-a)\phi\left[\frac{1}{|t|} \sum_{t \in \mathcal{N}(\bar{v})} h_u, h_{\bar{v}}\right] \\ &\approx \phi\left[\frac{1}{|t|} \sum_{t \in \mathcal{N}(\bar{v})} h_u, h_{\bar{v}}\right], \quad (a = \frac{|X_{ori}|}{|X_{syn}| + |X_{ori}|} \rightarrow 0)\end{aligned}$$

The whole representation of the minority class is dominated by the synthesized minority node. To the model, the above issue results in

$$\begin{aligned}&\mathbb{E}_{(u, c_{min}) \sim \mathcal{D}'_{tr}} [\mathcal{L}(\hat{f}_\theta(u)), c_{min}] \\ &= \mathbb{E}_{(v, c_{min}) \sim \mathcal{D}'_{tr}} [\mathcal{L}(\hat{f}_\theta(v)), c_{min}] + \mathbb{E}_{(\bar{v}, c_{min}) \sim \mathcal{D}'_{tr}} [\mathcal{L}(\hat{f}_\theta(\bar{v})), c_{min}] \\ &\approx \mathbb{E}_{(\bar{v}, c_{min}) \sim \mathcal{D}'_{tr}} [\mathcal{L}(\hat{f}_\theta(\bar{v})), c_{min}]\end{aligned}$$

$\mathcal{D}'_{tr}$  denotes the balanced training set after node mixup, and  $u \in \mathcal{D}'_{tr}$ . Therefore, the classification ability of the

model for the minority class tends to be completely trained by the synthesized node.  $\square$

## 4 PRELIMINARIES

In this section, we introduce the notation and core concepts used in this paper. The overview of GNN for node classification and problem definition is also introduced here.

### 4.1 Notation and Concept

In this paper, we focus on the node classification task performed on an undirected graph  $\mathcal{G} = (\mathcal{V}, \mathcal{X}, \mathcal{A}, \mathcal{Y})$ , where  $\mathcal{V} = \{v_1, v_2, \dots, v_n\}$  denotes the set of  $n$  nodes. The node features are represented by the matrix  $\mathcal{X} \in \mathbb{R}^{n \times d}$ , where  $d$  is the dimensionality of the feature space, and  $\mathcal{X}_i$  (the  $i$ -th row of  $\mathcal{X}$ ) corresponds to the feature vector of node  $v_i$ . The graph structure is encoded in the adjacency matrix  $\mathcal{A} \in \mathbb{R}^{n \times n}$ . The set of class labels is denoted by  $\mathcal{Y} = \{1, 2, \dots, c\}$ , comprising  $c$  classes, where  $\mathcal{Y}_i$  represents the  $i$ -th class, and  $\mathcal{Y}(v_i)$  denotes the label assigned to node  $v_i$ . We also use  $v_{i,j}$  to refer to the node  $v_i$  with the label  $j$ . Furthermore, we define  $\mathcal{N}(v_i)$  as the set of one-hop neighbors of the node  $v_i$ . Additionally, we define the imbalance ratio  $\rho$  as the ratio of the number of nodes in the most frequent class to the number of nodes in the least frequent class, given by  $\rho = \frac{|\{v \in \mathcal{V} | \mathcal{Y}(v) = \mathcal{Y}_{most\ freq}\}|}{|\{v \in \mathcal{V} | \mathcal{Y}(v) = \mathcal{Y}_{least\ freq}\}|}$ .  $\mathcal{Y}_{most\ freq}$  denotes the class with the highest frequency of occurrence, that is, the class with the largest quantity.  $\mathcal{Y}_{least\ freq}$  denotes the class with the least frequency of occurrence. This ratio provides a measure of the class imbalance in the graph. Moreover, GraphIFE leverages both features to address the challenges: 1) invariant features, which remain stable across different domains or structures and preserve predictive semantics under varying conditions; and 2) environment features vary across domains or graph structures but are not causally related to the prediction target.

### 4.2 GNN for Node Classification

Node classification is one of the fundamental tasks in graph-based machine learning, where the objective is to predict the labels of nodes based on their features and the graph topology. Given a graph  $\mathcal{G} = (\mathcal{V}, \mathcal{X}, \mathcal{A}, \mathcal{Y})$ , and a set of labeled nodes  $\mathcal{V}_L \subset \mathcal{V}$ , the goal is to infer the labels of the remaining unlabeled nodes  $f(\mathcal{X}, \mathcal{A}) \rightarrow \hat{\mathcal{Y}} \in \mathbb{R}^{N \times C}$ .

GNNs have emerged as powerful models for the node classification task by effectively combining node features with topological information through message passing mechanisms. At each layer, a node aggregates information from its neighbors and updates its representation. For a given node  $v$ , its representation  $h_v^{(l)}$  at the  $l$ -th layer of GNN is updated according to the following formulation:

$$h_v^{(l)} = \text{UPDATE}\left(h_v^{(l-1)}, \text{AGG}\left(\left\{h_u^{(l-1)} \mid u \in \mathcal{N}(v)\right\}\right)\right),$$

where  $h_v^{(l)}$  denotes the representation of node  $v$  at the  $l$ -th layer, and  $h_v^{(l-1)}$  is the representation from the previous layer. The function AGG performs an aggregation over the set of neighboring node representations  $\left\{h_u^{(l-1)} \mid u \in \mathcal{N}(v)\right\}$ , where  $\mathcal{N}(v)$  denotes the set of immediate neighbors of node

$v$ . The UPDATE function then combines the node’s previous representation  $h_v^{(l-1)}$  with the aggregated neighborhood information to produce the updated embedding  $h_v^{(l)}$ . It is noticed that the initial node representation is defined as  $h_v^{(0)} = X_v$ , where  $X_v$  is the input feature vector of the node  $v$ .

After computing the final-layer node embeddings, a projector is applied to map each embedding to a prediction vector  $\hat{y}_i$  over the target classes. The model is then trained using cross-entropy [13] to compute over the labeled nodes in the training set  $V_{\text{train}}$ :

$$\mathcal{L} = \frac{1}{|V_{\text{train}}|} \sum_{i \in V_{\text{train}}} \text{CrossEntropy}(\hat{y}_i, y_i), \quad (2)$$

where  $y_i$  denotes the ground-truth label of node  $i$ , and  $\hat{y}_i$  is the predicted class label output by the model.

### 4.3 Problem Definition

The primary objective of imbalance graph node classification is to address the class imbalance problem by synthesizing minority class nodes, thereby creating a more balanced graph structure and mitigating the detrimental effects of class imbalance on the original graph  $\mathcal{G}$ . To achieve this, a data augmentation strategy generates an augmented graph  $\mathcal{G}'$ . This augmented graph is then used as input for a GNN, that performs a standard node classification task. By leveraging the augmented graph  $\mathcal{G}'$ , the GNN is able to learn more robust and balanced node representations. In this paper, GraphIFE extracts the invariant feature of both synthesized and original nodes to mitigate the inconsistent quality of the synthesized nodes.

## 5 METHODOLOGIES

This section details the GraphIFE architecture, including its core components and the employed training strategies. GraphIFE is a GNN model designed within a Generative Adversarial Network (GAN) framework. It comprises two key components: an invariant feature extractor and an environmental feature extractor. The overall architecture of the framework is depicted in Fig. 2.

### 5.1 Implementations of GraphIFE

GraphIFE consists of the following components: (1) a two-layer GNN that encodes the input graph data into node-level embeddings; (2) an invariant feature extractor, which extracts invariant features from the embeddings; (3) an environment feature extractor, which extracts the environment features from the embeddings; (4) a gated augmentor, which employs a gating mechanism to adaptively combine the invariant and environmental features for data augmentation; and (5) a projector, which maps the augmented features to the output space for downstream tasks. Note that the data augmentation strategy draws partial inspiration from AIA [24]. While GraphIFE performs feature-level augmentation by introducing controlled noise to node attributes, AIA operates at the graph-level.

We detail the architecture of the feature extractor and describe the complete process of feature extraction within the proposed framework. The invariant feature extractor and

environment feature extractor share a common architectural framework  $M$ , yet maintain independent parameterizations through  $\theta_I$  and  $\theta_E$ , respectively. Each extractor is optimized according to distinct objective functions that align with its specialized roles in feature representation. The architecture of the feature extractor is based on a one-layer GNN denoted as  $f'$ . Given an imbalanced input graph  $\mathcal{G}$ , a GNN encoder  $f$  first processes the input to generate node representations  $Z$ . These representations are then utilized to synthesize new nodes and select appropriate neighbors, resulting in a transformed and more balanced graph  $\mathcal{G}'$ , from which balanced node representations  $Z'$  are derived. Subsequently, the feature extractor  $M$  is applied to both the original and synthesized nodes in  $Z'$  to extract the final set of features  $\mathcal{F}$ .

The overall feature extraction process can be formally summarized as follows:

$$Z = f(\mathcal{G}), \quad Z' = \text{Node Mixup}(Z), \quad \mathcal{F} = f'(Z').$$

It is important to note that Node Mixup refers to the entire balancing procedure, which encompasses both node synthesis and neighbor selection.

### 5.2 Invariant Feature Extractor

The invariant feature extractor is employed to capture the stable, environment-invariant features of each node, thereby mitigating the potential quality inconsistency arising from synthesized nodes. Incorporating the invariant feature extractor enhances the model’s capability to effectively distinguish minority class nodes during training. The whole process can be summarized as:  $\mathcal{F}_I = f'_I(\text{Node Mixup}(f(\mathcal{G})))$  where  $f(\mathcal{G})$  denotes the initial encoding of the input graph, and  $\text{Node Mixup}(\cdot)$  represents the node synthesis and neighbor selection process. Subsequently, the invariant feature representation  $\mathcal{F}_I$  is passed through a projector to generate the predicted outputs. These predictions are then compared against the ground-truth labels using the loss function, yielding the invariant feature loss defined as:

$$\mathcal{L}_{IF} = -\frac{1}{n} \sum_{i=1}^n y_i \log \text{Proj}(f'_{\theta_I}(\text{NodeMixup}(f(\mathcal{G}))), \quad (3)$$

Here  $n$  denotes the number of samples,  $y_i$  represents the ground-truth, and  $\text{Proj}$  denotes a projector which is applied to map each embedding to a prediction vector.

**Representation alignment.** For the minority class, another critical challenge lies in the quality disparities of synthesized node representations during training. This variance can hinder model stability and reduce the effectiveness of synthesized nodes in mitigating class imbalance. To address this issue, we propose a representation alignment mechanism. Specifically, GraphIFE computes an adaptive weight for the invariant feature loss associated with each node. This weighting strategy mitigates representation variance within the minority class, thereby enhancing the consistency and quality of the synthesized node representations. GraphIFE first computes the mean feature representation for each class. Subsequently, it calculates the similarity score  $S_i$  between each intra-class node and its corresponding class mean. To mitigate the quality disparities, those with similarity scores below the class-wise average similarity  $S_m$

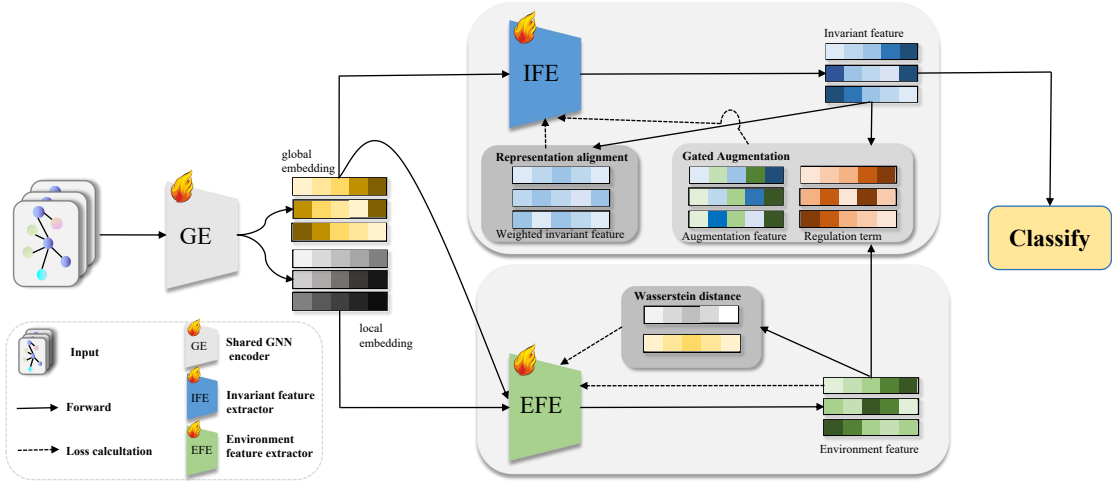


Fig. 2. The overview of the GraphIFE framework. The explanation of the notation used in the Figure is located in the bottom left. The training process consists of two distinct phases: (1) the training of the invariant feature extractor, and (2) the training of the environment feature extractor. Initially, the input imbalanced graph is processed through a shared GNN encoder, which simultaneously generates both local node embeddings and global graph embeddings. In phase (1), the invariant feature  $\mathcal{F}_I$  of the global embeddings is extracted by IFE; Then, the EFE extracts the environment features  $\mathcal{F}_E$  of the graph.  $\mathcal{F}_I$  and  $\mathcal{F}_E$  are combined through the gated augmentor to produce mixed features  $\mathcal{F}_m$ . The final loss computation incorporates both  $\mathcal{F}_m$  and  $\mathcal{F}_I$ , where the invariant feature loss undergoes representation alignment postprocessing. In phase (2), the environment feature  $\mathcal{F}_E$  of global embedding is extracted by EFE. Then, the local and global embedding both calculate the Wasserstein distance with  $\mathcal{F}_E$ . The final loss function incorporates both  $\mathcal{F}_E$  and Wasserstein distance results.

are assigned a weight of  $1 + (S_m - S_i)$ . This adaptive weighting scheme enables the model to focus more on intra-class nodes with higher representational variance. The weight  $W$  assigned to each node is defined as follows:

$$w_i = \begin{cases} 1, & S_i \geq S_m \\ 1 + (S_m - S_i), & S_i < S_m. \end{cases} \quad (4)$$

Finally, the representation alignment invariant loss is computed as  $\mathcal{L}'_{IF} = \mathcal{L}_{IF} \odot W$ , where  $\odot$  denotes the Hadamard product.

**Neighbor sampling.** Neighbor sampling is a strategy used to determine the set of nodes to which a newly synthesized node, denoted as  $\bar{v}$ , should be connected. The primary objective of this approach is to expose minority-class nodes to a more diverse set of structural and semantic neighborhoods. In this work, we construct the adjacent node distribution  $p(u | \bar{v})$  following the approach proposed in GraphENS [18]. In addition, we extend this formulation by incorporating the neighbor label distribution (NLD), which captures the label distribution within a node's local neighborhood. While conventional approaches account only for first-order neighborhood frequencies, they fail to leverage the structural information encoded in the NLD. We argue that incorporating NLD is crucial for constructing a more informative and balanced sampling distribution, as it potentially addresses the neighbor memorization problem highlighted in GraphENS, wherein the model tends to overfit to the labels of frequently encountered neighbors. We formally define the NLD as follows:

**Definition 2.** The neighbor labels distribution (NLD), represented as  $\mathcal{D} \in \mathbb{R}^{|\mathcal{V}| \times c}$ , quantifies the label distribution within each node's neighborhood. It is defined as:

$$\mathcal{D}_i = \bigcup_{j \in \mathcal{Y}} \{v \in \mathcal{N}(v_i) | j = \mathcal{Y}(v)\}. \quad (5)$$

$\mathcal{D}_i$  denotes the set of neighbor labels distribution of  $v_i$ , and  $\mathcal{D}_{i,j}$  denotes the element in  $\mathcal{D}_i$  where class =  $j$ .

Specifically, GraphIFE calculates the class average NLD ratio  $O^i_{ave}$ , and the identical label proportion  $O^i$  of each node, where  $i$  denotes the  $i$ -th class. Then, GraphIFE utilizes Min-Max normalization to calculate the NLD weights, which are then integrated into the adjacent node distribution. The NLD weight  $W_{NLD}$  process can be represented as:

$$w^i_{NLD} = \frac{O^i_{ave} - O^i_{min}}{O^i_{max} - O^i_{ave}}, \quad w^i_{NLD} \in [0, 1]. \quad (6)$$

The intuition is that the closer the vectors in space are, the more correlated they are [45]. Finally, we have the brand new adjacent node distribution  $p'(u | v_{mixed}) = p(u | v_{mixed}) \odot W^i_{NLD}$ . It is noteworthy that GraphIFE also adopts duplicated neighbors [18] as an initial warm-up strategy.

### 5.3 Environment Feature Extractor

The environment feature extractor is used to obtain the environment features of each node. These extracted features are subsequently employed to introduce controlled perturbations that challenge the model, thereby enhancing its capacity to discern class boundaries with greater precision, particularly for minority classes. Specifically, the environment feature extractor derives the embedding representation of environment features within the latent space, formally expressed as  $\mathcal{F}_E = f'_E(\text{Node Mixup}(f(\mathcal{G})))$ . The extracted representation  $\mathcal{F}_E$  is then passed through a projector to generate the corresponding predictions. These predictions are then compared against the ground-truth labels using the loss function, yielding the environment feature loss defined as:

$$\mathcal{L}_E = -\frac{1}{n} \sum_{i=1}^n y_i \log \text{Proj}(f'_{\theta_E}(\text{NodeMixup}(f(\mathcal{G}))). \quad (7)$$

Additionally, the extracted environment feature  $\mathcal{F}_E$  is utilized to compute the Wasserstein distance between the local representation  $R_{local}$  (encodes the structural information of a target node and its one-hop neighborhood) and the global representation  $R_{global}$  (captures the node’s topological characteristics within the entire graph).

$$\mathcal{L}_{DS} = \text{DS}(\mathcal{F}_E, R_{local}) + \text{DS}(\mathcal{F}_E, R_{global}). \quad (8)$$

Here,  $D_S(\cdot, \cdot)$  denotes the function used to compute the Wasserstein distance. The underlying intuition of the objective function is to encourage the extracted environment features to diverge from both the local structural patterns of individual classes and the global structural characteristics of the entire graph. This design aims to mitigate the impact of topological imbalance by promoting structural independence in the generated environmental features. The overall training objective of the environmental feature extractor can be formulated as:

$$\mathcal{L}_{EFE} = -\mathcal{L}_E + d\mathcal{L}_{DS}. \quad (9)$$

It is important to note that  $d$  is a hyperparameter. The objective of this formulation is to enhance the identification of environmental features. Specifically, the objective encourages the model to extract diverse environmental representations that remain consistent with the original data distribution.  $\mathcal{L}_E$  promotes the extraction of environment features that diverge from the invariant, stable representations, thereby introducing variability. In contrast,  $\mathcal{L}_{DS}$  guides the model to maintain alignment with the underlying data distribution while capturing subtle and latent structural variations. Through joint optimization of these complementary objectives, the model learns more generalized and robust feature representations that account for inherent environmental heterogeneity.

## 5.4 Gated Augmentor

To further enhance the model’s discriminative capability, GraphIFE incorporates a data augmentation strategy. Specifically, the augmentor generates an augmented feature representation, denoted as  $\mathcal{F}_m$ , by proportionally mixing invariant features with environment features. This combination enables the model to learn from a richer set of representations, thereby improving its ability to generalize across diverse and imbalanced graph structures. However, determining the optimal proportion for mixing invariant and environment features is non-trivial. To address this challenge, GraphIFE employs a gated augmentor module, denoted as  $f_G$ , which is designed to learn the appropriate mixing ratio.

The gated augmentor introduces controlled noise (environment feature) into the invariant features to perturb the model’s discriminative capability and encourage generalization. Specifically, the augmentor incorporates a learnable linear layer that takes the environment features as input to produce a gating value  $g$ . This gating value is then passed through a sigmoid activation function  $\sigma$  to compute the mixing proportion. Finally, the gated augmentor generates the augmented feature  $\mathcal{F}_m$  by combining the invariant and environmental features according to the learned proportion.

The overall mechanism of the Gated Augmentor can be formally summarized as follows:

$$g = \sigma(f_G(F_I, F_E)), \quad \mathcal{F}_m = F_I + gF_E.$$

In the aforementioned data augmentation process, the model autonomously determines the extent to which environment features should be integrated into each feature dimension. During this process, the model dynamically learns dimension-specific weighting coefficients that govern the integration of environmental features into each feature representation. By doing so, the augmentor can mitigate issues such as non-convergence of the loss function or the dominance of environmental features that may result from direct, unregulated feature superposition. Subsequently, the data augmentation loss is computed to guide the model in learning robust and discriminative feature representations:

$$\mathcal{L}_{DA} = -\frac{1}{n} \sum_{i=1}^n y_i \log \text{Proj}(F_I + \sigma(f_G(F_I, F_E))F_E), \quad (10)$$

**Regulation.** During training, the gate value may become excessively large, causing the environmental features to dominate the representation and introduce noise. Conversely, if the gate value is too small, the environmental features may be effectively ignored, rendering the augmentation ineffective and limiting the model’s ability to leverage environmental information. To mitigate excessive influence from environmental features, we introduce a regularization term that encourages the gate values to remain close to zero, thereby minimizing unnecessary interference. Specifically, this regularization is implemented as an  $\ell_1$  sparsity constraint, denoted as  $g'$ .

Given that the invariant feature extractor must simultaneously optimize multiple loss functions for effective convergence, we employ Dynamic Weight Averaging (DWA) [46] to adaptively generate the weighting vector  $W_D = [w_{d1}, w_{d2}]$ . This approach enables balanced training and promotes more stable and efficient model convergence. The overall training objective for the invariant feature extractor can be formally expressed as follows:

$$\mathcal{L}_{IFE} = w_{d1}\mathcal{L}'_{IF} + w_{d2}\mathcal{L}_{DA} + \alpha g', \quad (11)$$

where  $w_{d1}$  and  $w_{d2}$  denote the adaptive weights generated by DWA, and  $\alpha$  is a hyperparameter that controls the influence of the regularization term  $g'$ .

## 5.5 Theoretical Analysis

In this section, we illustrate how GraphIFE mitigates the feature inconsistency of the synthesized node from a theoretical perspective. To mitigate the feature inconsistency issue of the synthesized node, GraphIFE would extract the invariant feature of nodes, including the original training set and the synthesized node. GraphIFE doesn’t change the quantity relationship of the original and the synthesized node. It decouples the quality and quantity of nodes and mitigates the feature inconsistency issue by making the node representation of intra-class as consistent as possible. Although  $P(X_{syn}|Y_{min}) \neq P(X_{ori}|Y_{min})$ , GraphIFE achieve  $P(R_{syn}|Y_{min}) \approx P(R_{ori}|Y_{min})$  in embedding space,  $R$  denotes representation.

In summary, GraphIFE would affect the representation of nodes as follows:

*Proof:* The representation after GraphIFE. Given  $v \in V_{ori}$ ,  $\bar{v} \in V_{syn}$ . To the representation of the minority class, we have:

$$h_v = a\phi\left[\frac{1}{|u|} \sum_{u \in \mathcal{N}(v)} h_u, h_v\right] + (1-a)\phi\left[\frac{1}{|t|} \sum_{t \in \mathcal{N}(\bar{v})} h_u, h_{\bar{v}}\right]$$

$$\approx \phi\left[\frac{1}{|t|} \sum_{t \in \mathcal{N}(\bar{v})} h_u, h_{\bar{v}}\right], \left(a = \frac{|X_{ori}|}{|X_{syn}| + |X_{ori}|} \rightarrow 0\right)$$

In GraphIFE, it optimizes  $\phi\left[\frac{1}{|y|} \sum_{y \in \mathcal{N}(x)} h_u, h_x\right]$ , which is the representation of AGG in message-passing mechanism, by NLD weight. It also utilizes different strategies to optimize  $h_x$ , which is the representation of the node itself.

To simplify the representation, we set  $\Phi(x) = \phi\left[\frac{1}{|y|} \sum_{y \in \mathcal{N}(x)} h_u, h_x\right]$ . In GraphIFE we have  $\Phi_{IF}(V) \approx \Phi(V_{syn}) \approx \Phi(V_{ori})$ . Under ideal conditions, we can think that  $\Phi_{IF}(V) = \Phi(V_{syn}) = \Phi(V_{ori})$ . Thus, the representation of the minority class can be represented as:

$$h_{v_{min}} = a\Phi(v) + (1-a)\Phi(\bar{v})$$

$$\approx \Phi(\bar{v})$$

$$\approx \Phi_{IF}(v).$$

To the model, we have:

$$\mathbb{E}_{(u,y) \sim \mathcal{D}'_{tr}}[\mathcal{L}(f(u), y)]$$

$$= \mathbb{E}_{(v,y) \sim \mathcal{D}'_{tr}}[\mathcal{L}(f'_I(v), y)] \cup \mathbb{E}_{(\bar{v},y) \sim \mathcal{D}'_{tr}}[\mathcal{L}(f'_I(\bar{v}), y)]$$

$$\approx \mathbb{E}_{(v,y) \sim \mathcal{D}'_{tr}}[\mathcal{L}(f'_I(v), y)]$$

That is, with the help of GraphIFE, the representation of synthesized and non-synthesized nodes can be captured by their invariant feature. Consequently, the model is not affected by the quality and inconsistent distribution of nodes, preventing confusion in the GNN.  $\square$

## 6 EXPERIMENTS

In this section, we present a comprehensive empirical evaluation of GraphIFE’s performance on class-imbalanced node classification tasks. The code is publicly available at <https://github.com/flzeng1/GraphIFE>.

### 6.1 Datasets and Settings

**Datasets.** We evaluate the effectiveness of GraphIFE on six benchmark datasets, encompassing both citation networks, Amazon-based co-purchasing, and collaboration graphs. The citation network datasets include (1) Cora, a network in which nodes represent scientific publications and edges

denote citation relationships between them; (2) CiteSeer, a similarly structured network with a different scale and statistical properties; and (3) PubMed, a larger citation graph focused on biomedical literature. These datasets are sourced from [25]. The Amazon datasets consist of (4) Photo and (5) Computer, both of which are product co-purchasing networks derived from Amazon, where nodes represent products and edges indicate frequently co-purchased item pairs. Additionally, we include the (6) CS dataset, a collaboration network extracted from the Microsoft Academic Graph, where nodes represent authors and edges denote co-authorships [14]. For experimental settings, we follow the Long-Tail setup for citation networks in [18], and adopt the step-setting configuration for the Amazon datasets, as introduced by [17]. Detailed statistics of all datasets are provided in Table 1.

**Baselines.** We evaluate the performance of GraphIFE by comparing it against baseline methods across three widely used GNN backbones: GCN [27], GAT [28], and GraphSAGE [26]. The comparison includes the following methods: (1) Reweight, which applies class-balanced reweighting by adjusting loss weights inversely proportional to class frequencies; (2) Upsampling, which directly replicates samples from the minority class to balance the dataset; (3) GraphSMOTE [11], which generates synthetic minority nodes by interpolating features of two nodes from the same minority class; (4) GraphENS [18], which creates new minority nodes by merging the ego-networks of minority nodes with those of randomly selected nodes; (5) TAM [22], which compares the structural connectivity patterns of each node with a class-averaged counterpart and adaptively adjusts the classification margin accordingly; (6) ReNode [20], which reduces the contribution of nodes near class boundaries by down-weighting their loss based on topological proximity; and (7) BAT [19], which addresses topological imbalance by applying dynamic topological augmentation during training. In our experiments, we specifically adopt the BAT0 variant. (8) GNN-CL [47] incorporates curriculum learning by adaptively generating interpolated nodes and edges, while jointly optimizing graph classification loss and metric learning. We set the class imbalance ratio to  $\rho = 100$  for the citation network datasets (Cora, PubMed, and CiteSeer), and  $\rho = 80$  for the Amazon datasets (Amazon-Photo, Amazon-Computer, and CS).

**Evaluation metrics.** We describe the evaluation metrics used to assess model performance across different datasets. Specifically, three metrics are employed: (1) Accuracy (Acc.), which measures the proportion of correctly classified samples relative to the total number of samples; (2) Balanced Accuracy (bAcc.), which accounts for class imbalance by computing the average recall across all classes, thereby providing a more equitable evaluation in imbalanced settings; and (3) F1 Score (F1), defined as the harmonic mean of precision and recall, which offers a balanced assessment of the model’s ability to correctly identify both positive and negative instances. These three metrics are consistently applied to evaluate the performance of all baseline methods across the considered datasets.

TABLE 1  
Statistics of benchmark datasets.

Dataset	Nodes	Edges	Features	Classes
Cora	2,078	10,556	1,433	7
CiteSeer	3,327	9,104	3,703	6
PubMed	19,717	88,648	500	3
Photo	7,650	119,081	745	8
Computer	13,752	245,861	767	10
CS	18,333	81,894	6,805	15

TABLE 2  
The parameter settings of GraphIFE applied across different GNN backbones and datasets in the main results.

Dataset		Cora-LT	Citeseer-LT	PubMed-LT	Photo-ST	Computer-ST	CS-ST
GCN	Distance ratio $d$	0.5	0.5	0.5	0.5	0.5	0.5
	Regulation ratio $\alpha$	0.5	0.5	0.5	0.5	0.1	0.1
	IFE learning rate $r_1$	1e-3	1e-3	1e-3	1e-3	1e-3	1e-3
	EFE learning rate $r_2$	1e-2	1e-2	1e-2	1e-2	1e-2	1e-2
	DWA temperature $t$	2	2	2	2	2	2
	Warmup $\omega$	10	10	5	100	100	1
GAT	Distance ratio $d$	1	1	1	2	1	2
	Regulation ratio $\alpha$	1	0.5	0.5	0.8	0.5	0.8
	IFE learning rate $r_1$	1e-2	1e-3	1e-2	1e-3	1e-3	1e-4
	EFE learning rate $r_2$	1e-2	1e-2	1e-2	1e-2	1e-2	1e-2
	DWA temperature $t$	1	2	2	2	2	1
	Warmup $\omega$	1	1	1	150	100	1
SAGE	Distance ratio $d$	0.5	0.5	0.5	0.5	0.5	0.5
	Regulation ratio $\alpha$	0.1	0.5	0.5	0.1	0.1	0.1
	IFE learning rate $r_1$	1e-2	1e-3	1e-3	1e-3	1e-3	1e-3
	EFE learning rate $r_2$	1e-2	1e-2	1e-2	1e-2	1e-2	1e-2
	DWA temperature $t$	1	2	2	2	2	2
	Warmup $\omega$	1	10	1	100	100	1

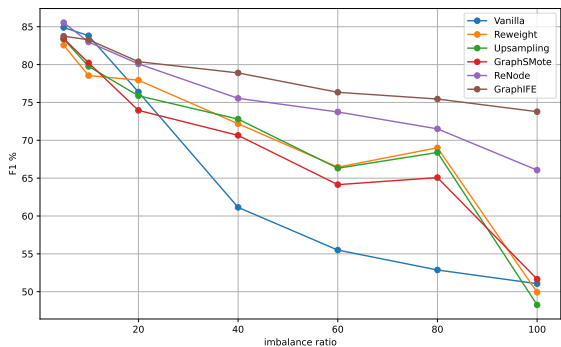


Fig. 3. Changing trend of F1-score with the increase of imbalance ratio on PubMed-LT with GCN.

## 6.2 Main Results

We illustrate the performance of GraphIFE in six different datasets compared with various baselines. It should be noted that the citation network datasets (Cora, CiteSeer, and PubMed) follow the LT class imbalance setting [18], while the Amazon datasets (Photo, Computer) and collaboration network datasets (CS) utilize the step class imbalance setting [20]. Additionally, the imbalance ratio  $\rho = 100$  in the LT class imbalance setting, while  $\rho = 80$  in the step class imbalance setting. The parameter settings of GraphIFE are summarized in Table 2. For all experiments, the feature dimension of each GNN is fixed at 256, and the number of attention heads in GAT is set to 8.

The performance of various baselines compared with GraphIFE on the citation networks is presented in Table 3. In the LT class imbalance setting, GraphIFE achieves the best performance in accuracy, balanced accuracy, and F1-score for both GCN and SAGE. Specifically, in GCN, GraphIFE attains improvements of 1.50% in accuracy, 3.15% in balanced accuracy, and 3.27% in F1-score on Cora-LT compared with GraphENS. Additionally, GraphIFE obtains 1.42% Acc, 1.47% bAcc, and 1.02% F1 improvement in Citeseer-LT compared with GraphENS. GraphIFE also obtains 0.09%

Acc, 2.70% bAcc, and 1.71% F1 improvement in PubMed-LT compared with GraphENS. In SAGE, GraphIFE only obtains a slight improvement compared with other baselines. While using GAT as the backbone, GraphIFE achieves the best performance in Cora-LT and PubMed-LT. In Citeseer, GraphIFE has a slight gap compared with GraphENS in bAcc. and F1, which  $\downarrow 0.01\%$  and  $\downarrow 0.20\%$ , respectively. Nevertheless, many baselines, like Reweight and Upsampling, struggle in the LT setting.

The performance of various baselines compared with GraphIFE on the Amazon datasets and collaboration network datasets is presented in Table 4. Under the step class imbalance setting, the results demonstrate that GraphIFE achieves competitive performance when implemented with both GCN and GAT, while attaining the best performance when combined with SAGE. In GCN, GraphIFE generally achieves the best performance, although it shows minor deficiencies on certain specialized metrics. For example, GraphIFE has slight gaps compared with GraphENS,  $\downarrow 0.53\%$  of bAcc. in Photo;  $\downarrow 0.12\%$  of F1 in Computer and  $\downarrow 0.04\%$  of bAcc. in CS. In GAT, GraphIFE achieves the second best performance with slight gaps compared with other baselines. In SAGE, GraphIFE achieves the best performance across all baselines, especially obtaining 1.71% and 1.95% improvement of Photo-ST in bAcc. and F1, respectively; 1.42% and 1.41% improvement of Computer-ST in bAcc. and F1; 1.23% improvement of CS-ST in Acc. It is noticed that BAT especially struggles in Amazon datasets and collaboration network datasets. The above experiments show that GraphIFE is an effective method for solving the supervised graph imbalance node classification task.

## 6.3 Results on Large-scale Graph

The class imbalance problem is also prevalent in real-world large-scale graphs. To evaluate the generalizability of GraphIFE, we test its performance on a naturally imbalanced large-scale graph. Specifically, we conduct experiments on the OGB-Arxiv dataset [48], which exhibits severe class imbalance, with imbalance ratios of 775 in the training set, 2,282 in the validation set, 2,148 in the test set, and 942 overall. Due to the large scale of OGBN-Arxiv,

TABLE 3

Imbalance node classification result of GraphIFE compared with other baselines. We set the imbalance ratio in an extreme setting ( $\rho = 100$ ) with standard errors five times. The best-performing result is highlighted in **bold**, while the second-best result is indicated with underlining.

	Dataset	Cora-LT			CiteSeer-LT			PubMed-LT		
		$\rho=100$	Acc.	bAcc.	F1	Acc.	bAcc.	F1	Acc.	bAcc.
GCN	Vanilla	73.60±0.43	64.13±0.71	63.78±0.68	54.56±0.41	47.79±0.38	43.17±0.57	69.48±0.98	56.54±0.79	51.06±0.73
	Reweight	72.38±0.18	64.86±0.28	65.23±0.29	54.60±0.71	48.09±0.81	43.67±1.17	67.90±0.73	55.26±0.58	49.92±0.50
	Upsampling	71.64±0.49	63.63±0.68	63.97±0.85	54.62±0.66	48.03±0.68	43.53±1.01	65.76±0.15	53.54±0.12	48.26±0.11
	GraphSMOTE	71.48±0.21	62.94±0.22	63.39±0.17	53.80±0.17	47.25±0.19	42.91±0.37	67.90±0.24	55.84±0.18	51.66±0.42
	GraphENS	76.64±0.40	71.29±0.69	71.01±0.67	62.22±0.48	56.16±0.59	55.09±0.72	76.90±0.30	71.11±1.23	72.07±1.14
	BAT	75.32±0.49	66.57±0.73	66.09±0.88	57.46±0.61	51.00±0.66	47.50±1.04	68.58±0.50	56.17±0.47	51.55±0.67
	GNNCL	70.88±0.32	60.20±0.57	58.13±0.70	52.70±0.21	46.14±0.21	40.96±0.35	43.24±2.42	35.31±1.89	23.77±3.20
	ReNode	70.82±1.04	63.08±1.46	64.95±1.78	53.90±1.63	49.94±1.17	48.68±1.42	68.76±1.32	68.14±1.50	66.06±1.42
	TAM	70.12±1.27	62.29±1.65	64.10±2.18	56.40±1.31	52.38±1.04	51.72±1.03	68.86±1.68	66.70±1.86	65.74±1.86
	<b>GraphIFE</b>	<b>78.14±0.23</b>	<b>74.44±0.22</b>	<b>74.28±0.26</b>	<b>63.64±0.85</b>	<b>57.63±0.65</b>	<b>56.11±0.62</b>	<b>76.96±0.44</b>	<b>73.81±1.19</b>	<b>73.78±0.99</b>
GAT	Vanilla	73.54±0.33	64.44±0.53	64.06±0.77	56.80±0.32	50.23±0.29	46.65±0.35	70.55±0.25	57.40±0.20	51.92±0.18
	Reweight	73.62±0.79	66.19±1.19	66.54±1.37	53.92±0.22	47.40±0.22	41.91±0.43	63.16±0.42	51.45±0.34	46.28±0.34
	Upsampling	72.94±0.67	65.90±0.96	66.19±1.09	54.46±0.20	47.92±0.19	42.78±0.29	64.10±0.28	52.21±0.23	47.04±0.23
	GraphSMOTE	73.76±0.51	66.23±0.63	67.07±0.92	54.90±0.16	48.23±0.16	43.78±0.32	67.82±0.43	55.91±0.52	51.96±0.85
	GraphENS	77.52±0.21	72.18±0.44	71.98±0.65	63.76±0.15	<b>57.62±0.22</b>	<b>56.27±0.33</b>	76.10±0.10	69.88±0.39	70.77±0.44
	BAT	76.24±0.17	67.55±0.26	65.69±0.17	57.50±0.52	50.70±0.55	47.10±0.82	64.52±1.84	52.54±1.48	47.29±1.54
	GNNCL	71.84±0.36	61.68±0.37	59.76±0.37	54.82±0.12	48.16±0.10	43.55±0.16	63.28±0.49	51.59±0.43	46.47±0.51
	ReNode	66.98±0.82	58.77±0.77	60.43±1.13	48.30±3.34	44.48±2.59	41.73±2.68	66.62±2.47	68.29±2.60	63.62±3.15
	TAM	66.84±1.15	58.78±1.14	59.75±1.37	54.88±2.38	51.21±1.72	49.34±1.90	66.94±3.28	68.11±3.45	64.15±4.00
	<b>GraphIFE</b>	<b>77.62±0.47</b>	<b>72.97±0.56</b>	<b>72.91±0.73</b>	<b>63.90±0.51</b>	<u>57.61±0.51</u>	<u>56.07±0.44</u>	<b>76.24±0.09</b>	<b>71.07±0.13</b>	<b>71.98±0.10</b>
SAGE	Vanilla	71.56±0.29	60.27±0.36	60.57±0.29	50.30±0.40	44.00±0.35	39.34±0.55	63.50±1.10	51.72±0.88	46.45±0.92
	Reweight	72.66±0.57	63.23±0.85	63.77±0.86	54.88±0.33	48.26±0.32	43.47±0.34	69.80±1.64	57.79±1.63	54.10±2.07
	Upsampling	71.62±0.66	62.24±0.85	62.76±0.95	54.98±0.25	48.44±0.17	44.04±0.19	73.44±0.93	63.20±1.72	62.04±2.31
	GraphSMOTE	73.32±0.84	64.11±0.96	64.86±0.91	54.02±0.35	47.78±0.37	44.56±0.55	73.60±1.46	63.85±1.85	63.66±2.41
	GraphENS	76.46±0.29	70.30±0.37	69.83±0.39	63.58±0.33	57.12±0.32	55.21±0.19	77.80±1.20	71.21±2.06	72.35±2.20
	BAT	76.68±0.53	69.72±0.73	70.39±0.84	56.70±0.54	50.81±0.59	46.56±0.84	70.58±0.42	57.59±0.27	52.50±0.18
	GNNCL	71.84±0.36	61.68±0.37	59.76±0.37	54.82±0.12	48.16±0.10	43.55±0.16	63.28±0.49	51.59±0.43	46.47±0.51
	ReNode	65.66±1.02	55.09±1.39	53.95±2.01	40.48±2.44	36.70±1.82	33.25±1.38	58.44±0.64	60.01±0.50	52.38±0.94
	TAM	66.08±0.76	56.70±0.98	56.31±1.41	56.56±2.36	52.19±1.70	51.53±1.70	58.00±1.12	59.46±0.91	52.02±1.56
	<b>GraphIFE</b>	<b>76.90±0.19</b>	<b>70.75±0.13</b>	<b>70.79±0.14</b>	<b>63.80±0.37</b>	<b>57.52±0.37</b>	<b>55.83±0.32</b>	<b>78.58±0.80</b>	<b>75.29±1.95</b>	<b>75.37±1.76</b>

GraphIFE encounters out-of-memory (OOM) issues during runtime. To address this limitation, we employ GraphIFE-Light, a simplified variant that reduces the complexity of the neighbor sampling strategy in node mixup. Specifically, GraphIFE-Light directly duplicates the neighbors of minority nodes during sampling, thereby reducing GPU memory consumption. However, such direct duplication may impair the message-passing mechanism of GNNs, as many nodes exhibit anomalous connectivity patterns within their class [22]. To compensate for this limitation, GraphIFE-Light incorporates a filtering mechanism that removes anomalous connectivity nodes during both training and node sampling stages. Concretely, it excludes nodes whose label proportion satisfies  $R^i < \epsilon$ , where  $\epsilon$  is a hyperparameter.

We apply GraphIFE-Light with GCN as the backbone. The baseline results are taken from GraphSHA [17] and the OGB leaderboard [48]. Experimental results are sum-

marized in Table 5, where “OOM” denotes out-of-memory errors. We report validation accuracy, test accuracy, balanced accuracy, and test F1 score. The results show that, except for test BAcc., GraphIFE-Light consistently outperforms all baselines. These findings demonstrate the effectiveness of GraphIFE-Light on large-scale graphs.

#### 6.4 Hyperparameter Analysis

In this section, we explore the influence of the main hyperparameter to the performance of different datasets. The imbalance ratio  $\rho$ , the distance ratio  $d$ , and the regulation ratio  $\alpha$  are analyzed in the subsequent section.

**Imbatio ratio analysis.** We analyze the impact of class imbalance ratio  $\rho$  on model performance, with particular focus on F1-score variations across different methods. The experiment is conducted in the PubMed-LT dataset with GCN as GNN backbone, and the  $\rho$  ranges from 5 to 100. As illus-

TABLE 4

Imbalance node classification results of GraphIFE compared with other baselines. We set the imbalance ratio in an extreme setting ( $\rho = 80$ ) with standard errors five times. The best-performing result is highlighted in **bold**, while the second-best result is indicated with underlining.

	Dataset	Photo-ST			Computer-ST			CS-ST		
		Acc.	bAcc.	F1	Acc.	bAcc.	F1	Acc.	bAcc.	F1
GCN	Vanilla	38.85±0.09	46.82±0.09	31.08±0.46	60.25±0.45	48.73±1.40	33.19±0.18	36.92±0.68	52.03±0.59	26.21±1.24
	Reweight	44.41±4.17	50.12±2.24	32.77±2.86	61.87±0.09	49.62±0.54	33.18±0.43	39.32±0.84	51.35±1.26	25.47±2.05
	Upsampling	42.98±3.84	48.96±1.98	32.19±2.15	61.77±0.12	50.06±0.56	33.29±0.28	39.66±2.25	52.39±1.67	27.80±2.73
	GraphSMOTE	45.91±3.79	50.40±1.96	32.09±2.41	61.83±0.09	50.47±0.38	33.78±0.40	39.86±1.37	52.23±0.85	26.56±1.28
	GraphENS	81.17±0.38	<b>83.40±0.42</b>	78.64±0.90	75.36±0.27	82.72±0.16	69.72±0.35	85.05±0.54	85.45±0.30	74.68±0.34
	BAT	38.47±0.19	46.41±0.11	30.34±0.50	61.15±0.09	45.64±0.06	26.82±0.05	32.53±0.07	47.84±0.24	18.74±0.39
	GNNCL	38.68±0.31	46.63±0.32	29.07±1.10	49.74±7.97	37.11±5.45	22.60±4.13	31.83±0.21	46.73±0.24	19.24±0.99
	ReNode	71.20±0.27	77.03±0.23	67.72±0.33	74.56±0.33	82.25±0.15	<b>70.70±0.71</b>	86.21±0.35	<b>86.64±0.13</b>	75.57±0.19
	TAM	66.96±0.39	72.04±0.39	63.41±0.44	68.85±0.44	74.96±0.55	63.62±1.10	84.16±0.55	84.54±0.17	72.49±0.24
	<b>GraphIFE</b>	<b>81.92±1.06</b>	<u>82.83±0.79</u>	<b>80.03±0.97</b>	<u>75.96±0.42</u>	<b>83.65±0.20</b>	<u>70.58±0.52</u>	<b>86.61±0.45</b>	<u>86.60±0.29</u>	<b>76.69±0.41</b>
GAT	Vanilla	39.55±0.04	47.54±0.04	25.33±0.09	62.66±0.31	48.56±1.88	32.62±3.11	43.66±2.82	58.14±2.47	34.99±4.01
	Reweight	61.78±0.5	60.73±0.09	47.89±0.26	62.92±0.05	46.80±0.06	29.72±0.11	43.62±1.52	54.44±1.28	30.40±2.01
	Upsampling	62.32±0.24	61.35±0.31	49.40±0.78	62.85±0.04	46.76±0.03	29.62±0.07	40.16±2.06	53.12±1.45	27.11±2.00
	GraphSMOTE	62.41±0.24	61.53±0.65	49.95±1.58	62.84±0.02	46.87±0.02	29.64±0.10	41.37±2.62	54.89±1.57	30.13±2.59
	GraphENS	<b>83.45±0.20</b>	<b>85.93±0.38</b>	<b>82.08±0.29</b>	76.20±0.50	<b>83.63±0.34</b>	<b>71.26±0.65</b>	87.54±0.31	<b>87.81±0.28</b>	<b>76.17±1.41</b>
	BAT	39.03±0.11	47.08±0.09	30.78±0.80	62.92±0.25	45.98±0.10	32.07±0.59	32.30±0.07	47.25±0.13	20.93±1.10
	GNNCL	39.87±0.71	47.90±0.77	30.73±0.70	60.95±1.85	42.37±4.25	28.53±1.96	32.79±0.36	47.74±0.75	18.66±1.02
	ReNode	66.96±1.33	66.75±1.27	63.90±1.10	64.36±0.82	66.08±0.70	55.52±1.67	85.53±0.73	81.25±0.71	66.17±1.16
	TAM	58.39±1.72	61.11±1.89	53.34±1.76	64.69±0.44	64.43±1.99	54.88±1.82	81.20±1.80	76.62±0.98	62.75±0.72
	<b>GraphIFE</b>	<u>83.15±0.18</u>	<u>84.62±0.41</u>	<u>81.48±0.23</u>	<b>76.50±0.55</b>	<u>83.25±0.64</u>	<u>70.86±0.63</u>	<b>88.15±0.76</b>	<u>87.14±0.80</u>	<u>74.43±2.24</u>
SAGE	Vanilla	43.37±1.51	49.62±0.78	29.58±1.35	63.46±0.19	46.89±0.11	29.91±0.17	43.49±1.04	56.44±0.66	32.04±1.15
	Reweight	54.31±2.35	56.52±0.95	41.88±1.75	61.47±0.62	49.12±1.32	34.27±0.20	53.18±1.39	61.52±0.78	40.91±1.43
	Upsampling	56.29±1.16	57.67±1.20	43.97±1.70	62.80±0.03	52.40±1.90	37.24±2.38	51.99±1.99	62.63±0.64	41.62±1.13
	GraphSMOTE	56.68±1.27	56.24±0.54	41.52±1.04	61.35±0.45	48.73±1.40	33.19±1.80	53.08±1.72	63.64±0.88	40.93±1.19
	GraphENS	81.87±0.38	83.40±0.42	78.64±0.90	72.51±0.35	79.16±0.71	65.44±0.72	85.61±0.55	86.53±0.24	75.05±0.74
	BAT	45.99±2.04	53.04±1.22	35.04±2.15	63.01±0.60	46.83±0.29	30.43±0.22	63.01±0.60	46.83±0.29	30.43±0.22
	GNNCL	39.44±0.09	47.10±0.10	28.56±0.78	60.10±1.21	44.82±0.91	26.83±0.54	39.48±1.23	52.97±0.52	28.06±1.06
	ReNode	56.82±0.86	64.25±0.97	49.47±0.64	69.70±0.72	74.90±0.13	62.89±0.77	79.83±0.24	81.83±0.19	68.60±0.12
	TAM	54.33±0.69	62.02±0.77	46.87±0.72	66.18±0.60	66.64±0.63	51.87±0.76	82.11±0.51	82.21±0.17	69.90±0.30
	<b>GraphIFE</b>	<b>82.02±0.57</b>	<b>85.11±0.65</b>	<b>80.59±0.44</b>	<b>73.17±0.46</b>	<b>80.58±0.88</b>	<b>66.85±0.81</b>	<b>86.84±0.85</b>	<b>87.19±0.69</b>	<b>75.98±1.32</b>

TABLE 5

Node classification results ( $\pm$ std) on large-scale naturally class-imbalanced dataset ogbn-arXiv. OOM indicates Out-Of-Memory.

Method	Val Acc.	Test Acc.	Test bAcc.	Test F1
Reweight	67.49±0.32	66.07±0.55	53.34±0.30	48.07±0.77
CB Loss	65.75±0.23	64.73±0.86	52.66±0.72	47.24±1.25
Focal Loss	67.36±0.24	65.93±0.58	53.06±0.21	48.89±0.72
ReNode	66.44±0.51	65.91±0.20	53.39±0.40	48.18±0.52
TAM (ReNode)	67.91±0.27	66.63±0.66	<b>53.40±0.24</b>	48.71±0.49
Upsample	70.53±0.08	69.55±0.37	46.82±0.07	45.49±0.20
GraphSmote	OOM	OOM	OOM	OOM
GraphENS	OOM	OOM	OOM	OOM
GraphIFE	OOM	OOM	OOM	OOM
<b>GraphIFE-Light</b>	<b>71.41±0.35</b>	<b>70.78±0.21</b>	53.06±0.17	<b>51.89±0.46</b>

trated in Fig. 3, we can observe that F1-scores exhibit statistically significant degradation as  $\rho$  increases. While GraphIFE does not achieve peak performance initially, it demonstrates remarkable robustness as  $\rho$  increases. GraphIFE maintains consistent performance stability under increasing imbalance

conditions, whereas competing methods show statistically significant F1-score degradation. These experimental results highlight GraphIFE’s robust performance under extreme class imbalance conditions.

**Distance ratio analysis.** We experiment to analyze the influence of the Wasserstein distance to the performance of the model. The parameter  $d$  governs the relative contribution of the Wasserstein distance between local and global representations in the environment feature training process. The experiment is conducted on Photo-ST dataset with GCN as a backbone by controlling the value of  $d$ , systematically examining the impact of parameter  $d$ . As shown in Fig. 4a and Fig. 4c, with a fixed  $\alpha$ , the overall accuracy generally exhibits an upward trend. However, for  $\alpha \in \{0.5, 0.6, 0.7\}$ , the accuracy first increases, then decreases, and subsequently rises again. In Fig. 4c, it is evident that larger values of  $d$  lead to better model performance. For instance, when

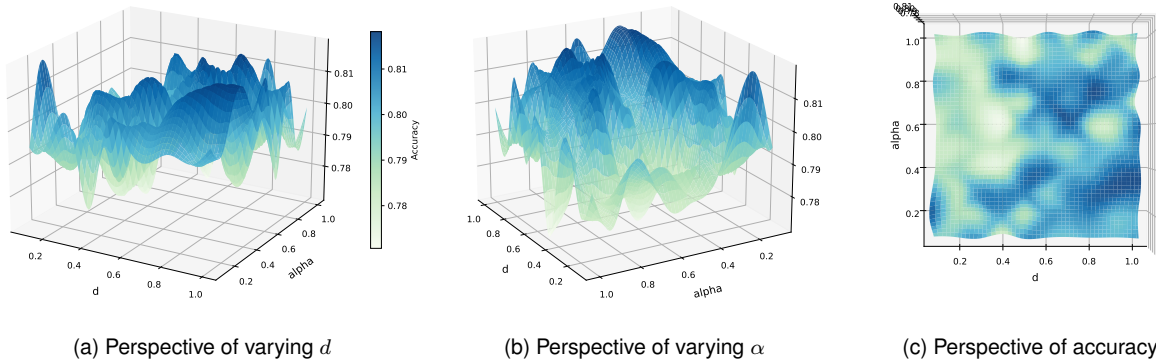


Fig. 4. The experiment results of exploring the combined effects of distance ratio  $d$  and regulation ratio  $\alpha$  on the performance of GraphIFE. The experiment is conducted on Photo-ST with GCN as the GNN backbone. Accuracy is utilized as the performance metric. The color denotes the performance change. The deeper the color, the better the performance.

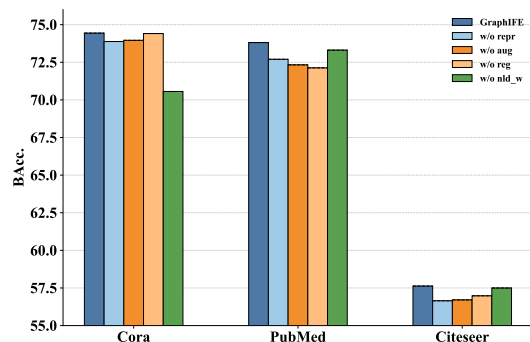


Fig. 5. Ablation study of different GraphIFE variants on three datasets.

$d > 0.5$ , the figure displays a deeper color, indicating higher accuracy.

**Regulation ratio analysis.** We conducted the experiment to analyze the regularization term’s impact within the invariant feature extractor.  $\alpha$  is the hyperparameter that controls the proportion of regulation. The experiment is conducted on the Photo-ST dataset with GCN as a backbone through controlling the value of  $\alpha$ . As shown in Fig. 4b and Fig. 4c, when  $d$  is fixed, the performance does not exhibit a clear linear trend with increasing  $\alpha$ . Instead, the overall results display a fluctuating pattern, characterized by an initial increase, followed by a decrease, and then a subsequent increase.

In summary, as illustrated in Fig. 4c, the closer a region is to the middle or lower-right side of the figure, the darker its color becomes, indicating improved performance. This suggests that combining a larger value of  $d$  with a moderate value of  $\alpha$  yields better overall results.

## 6.5 Ablation Study

This subsection presents an ablation study evaluating the individual contributions of GraphIFE’s core components. We assess model performance across three established benchmark datasets (Cora-LT, PubMed-LT, and Citeseer-LT) using GCN as the backbone and balanced accuracy as the evaluation metric. GraphIFE is employed as the baseline to

TABLE 6  
Classification accuracy for each class on Cora-LT.

Class Distribution	$C_0$ (0.5%)	$C_1$ (1.1%)	$C_2$ (2.4%)	$C_3$ (5.4%)	$C_4$ (11.6%)	$C_5$ (25.0%)	$C_6$ (54.0%)
Reweight	32.9	70.9	75.0	67.5	78.6	93.5	87.9
PC Softmax	29.7	78.0	70.9	66.2	81.2	93.8	82.5
CB Loss	31.3	74.7	72.8	69.2	81.9	94.0	83.4
Focal Loss	29.9	75.9	72.2	71.9	82.6	94.6	83.2
ReNode	35.9	73.6	72.8	66.9	83.9	95.1	88.1
Upsample	12.5	58.2	65.1	67.5	76.5	92.4	89.7
GraphSmote	22.2	66.4	68.9	62.1	79.4	93.4	89.4
GraphENS	37.7	72.2	73.2	63.5	74.6	94.7	82.3
TAM (G-ENS)	32.6	76.3	68.9	71.5	74.2	95.1	86.9
<b>GraphIFE</b>	<b>34.3</b>	<b>79.1</b>	<b>69.9</b>	<b>68.4</b>	<b>77.8</b>	<b>93.7</b>	<b>81.8</b>

facilitate comparative analysis with the component-ablated variants. The following variants of GraphIFE are considered: (1) “w/o repr”: GraphIFE without representation alignment during the training of the invariant feature extractor; (2) “w/o aug”: GraphIFE without data augmentation during the training of the invariant feature extractor; (3) “w/o reg”: GraphIFE without regulation during the training of the invariant feature extractor; and (4) “w/o nld\_w”: GraphIFE without neighbor label distribution weight  $W_{NLD}$  in the neighbor sampling process.

As illustrated in Fig. 5, the experimental results demonstrate that the complete GraphIFE consistently outperforms all invariants. The performance declines when eliminate the specific component of GraphIFE is eliminated. The ablation study reveals consistent performance degradation when removing individual components from GraphIFE, which demonstrates each component’s essential contribution to the framework’s overall effectiveness. The impact of different parts on performance varies in different datasets. w/o repr, w/o aug, and w/o reg obtain a notable decline in performance of the model. Especially without representation alignment, w/o repr  $\downarrow 0.56\%$ ,  $\downarrow 1.11\%$ ,  $\downarrow 0.98\%$  in Cora-LT, PubMed-LT, and Citeseer-LT, respectively, compared with GraphIFE. Without data augmentation, w/o aug  $\downarrow 1.48\%$  in PubMed-LT. The impact of  $W_{NLD}$  on performance varies with different datasets. This is mainly because of the different NLD of different datasets. For example,  $W_{NLD}$  is essential on Cora-LT, w/o nld\_w  $\downarrow 3.88\%$  on Cora-LT, while the performance degradation is relatively small on PubMed-

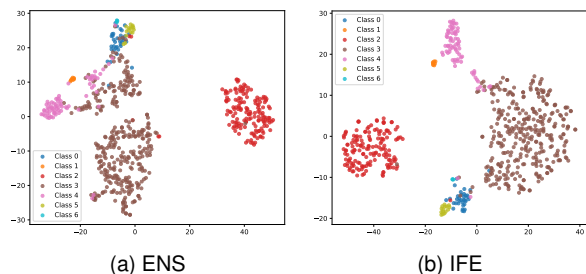


Fig. 6. Visualization.

LT and Citeseer-LT. In summary, GraphIFE demonstrates superior performance compared to all variants, while other variants have achieved varying degrees of performance degradation.

We further present a case study on per-class accuracy for baseline methods and GraphIFE with a GCN backbone on Cora-LT, as reported in Table 6. The results for other methods were sourced from a previous study [17]. GraphSmote yields only marginal improvements for minority classes compared to simple Upsampling, indicating that synthesizing nodes within minority classes alone is insufficient to substantially expand the decision boundary. In contrast, GraphENS achieves relatively high accuracy for minority classes; however, this improvement comes at the expense of reduced performance on major classes, suggesting that GraphENS may excessively generate minority nodes. GraphIFE demonstrates balanced performance across both minority and major classes, thereby narrowing the overall accuracy gap. Nonetheless, a performance drop is observed in classes  $C2$  and  $C6$ .

TABLE 7  
Complexity comparison of GraphIFE and different models.

	Dataset	Vanilla		GraphENS		GraphIFE	
		Time	Memory	Time	Memory	Time	Memory
GCN	Cora	00m 35s	6.67 MB	01m 00s	60.14 MB	01m 35s	178.34 MB
	CiteSeer	00m 36s	15.54 MB	01m 11s	127.84 MB	01m 35s	327.96 MB
	PubMed	01m 02s	3.28 MB	05m 38s	1511.28 MB	07m 40s	4668.59 MB
	Photo	01m 56s	3.99 MB	02m 24s	251.09 MB	04m 54s	858.26 MB
	Computer	03m 33s	4.11 MB	04m 17s	769.77 MB	09m 16s	2004.93 MB
	CS	02m 43s	27.74 MB	04m 05s	1828.91 MB	07m 32s	3404.69 MB
GAT	Cora	00m 32s	6.68 MB	00m 55s	60.15 MB	01m 57s	552.56 MB
	CiteSeer	00m 33s	15.55 MB	01m 05s	127.85 MB	02m 07s	544.51 MB
	PubMed	01m 15s	3.29 MB	06m 04s	1511.30 MB	12m 28s	6377.69 MB
	Photo	02m 16s	4.00 MB	02m 41s	251.10 MB	13m 14s	4224.71 MB
	Computer	04m 26s	4.13 MB	05m 15s	769.79 MB	28m 14s	8993.25 MB
	CS	03m 01s	27.76 MB	04m 28s	1828.92 MB	16m 00s	5590.39 MB
SAGE	Cora	00m 27s	13.26 MB	00m 53s	66.14 MB	01m 22s	288.08 MB
	CiteSeer	00m 38s	31.00 MB	01m 20s	143.30 MB	01m 56s	621.91 MB
	PubMed	00m 54s	6.23 MB	05m 23s	1554.23 MB	07m 15s	4673.54 MB
	Photo	01m 46s	7.90 MB	02m 26s	255.00 MB	04m 23s	1067.68 MB
	Computer	03m 31s	8.11 MB	04m 49s	773.77 MB	08m 54s	2486.06 MB
	CS	10m 19s	55.33 MB	14m 31s	1857.04 MB	07m 38s	8719.30 MB

## 6.6 Complexity Analysis

In this subsection, we analyze the time, peak GPU memory consumption, and calculate the time complexity of GraphIFE. We compare the complexity of our method with Vanilla and GraphENS to explore its efficiency and scalability. As shown in Table 7, GraphIFE consumes more time and memory compared with Vanilla and GraphENS for better comparison. In terms of the GNN backbone, GCN consumes the least amount of time and memory. GraphIFE consumes most memory on PubMed-LT and most time on CS-ST with

GCN as a backbone, while GAT consumes most resources because of its calculation of attention. GraphIFE consumes most time and memory on Computer-ST with GAT as the backbone.

Finally, we analyze the time complexity of GraphIFE in the training process. We first denote the number of nodes and edges in the dataset are  $n$  and  $e$ . Then, we formally denote the architectural parameters as follows: (1) Layer configurations,  $l$ ,  $l_{IF}$ ,  $l_{EF}$  denote the layers of the GNN backbone, invariant feature extractor, and environment feature extractor, respectively; (2) Hidden dimensions:  $d$ ,  $d_{IF}$ ,  $d_{EF}$  denote the dimensions of hidden layers in the GNN backbone, invariant feature extractor, and environment feature extractor, respectively; (3) Operational frequencies:  $s$  denotes the time of the node synthesis process.  $a$  denotes the time of the gated mixup mechanism.

Using the notation above, we first calculate (i) the time complexity of the invariant feature extractor, then (ii) the environment feature extractor, and finally (iii) the complexity of the entire training process. Specifically, to calculate (i), the time complexity of the invariant feature extractor training process includes: the calculation of invariant feature extraction  $O((dl + d_{IF}l_{IF})(n + e))$ ; the calculation of environment feature extraction  $O((d_{EF}l_{EF})(n + e))$ ; the regulation term  $O(n)$ ; and the calculation of representation alignment  $O(nd)$ . Note that the invariant feature extractor and the environment feature extractor share the same architecture, then  $d_{IF} = d_{EF}$  and  $l_{IF} = l_{EF}$ . The time complexity of the invariant feature extractor training process is  $O((n + e)(dl + 2d_{IF}l_{IF}) + a + n + s)$ . To calculate (ii), the complexity of the environment feature extractor training includes the calculation of environment feature extraction  $O((n + e)(dl + dl_{EF}))$  and the calculation of Wasserstein distance  $O(2nd)$ . Therefore, the time complexity of environment feature extractor training process is  $O((n + e)(dl + d_{EF}l_{EF}) + 2nd)$ . Finally, to calculate (iii), the overall time complexity of the full training process is  $O((n + e)(2dl + 3d_{EF}l_{EF}) + 2nd + a + n + s)$ .

## 6.7 Visualization and Limitation

As shown in Fig. 6, this section presents a visualization of node representations in embedding space using T-SNE. The visualization depicts the representation of nodes in the Cora-LT dataset before the final projector layer. We show the node representations for GraphENS and GraphIFE, respectively. Different colors denote different classes. In Fig. 6a, some confusion is observed in GraphENS classification; for example, the classification boundaries between classes pink, blue, brown, and yellow classes are unclear and even overlap. As shown in Fig. 6b, the boundaries issue has eased a lot in IFE while still existing, like the pink and brown overlap in the top right. In this paper, we found that the quality inconsistency issue exists in graph imbalance node classification, and proposed GraphIFE to tackle it. Our experimental results demonstrate that GraphIFE achieves effective performance. However, we also acknowledge and reflect on the limitations of our approach. The primary limitation is its substantial computational overhead. Due to the GAN framework, GraphIFE requires training an additional model for data augmentation to mitigate the topology

imbalance. While GraphIFE achieves better performance compared with other baselines, it incurs significantly higher computational costs than the vanilla approach. We expect to optimize GraphIFE’s computational efficiency while preserving its performance advantage.

## 7 CONCLUSION AND FUTURE WORK

In this paper, we explore the graph imbalance node classification problem and identify the quality inconsistency issue, where the feature of synthesized nodes may be out of distribution during the node synthesis process. To address this issue, we propose a GAN-like framework called GraphIFE, which leverages an invariant feature generator to extract the invariant features of both original and synthesized nodes and an environment feature extractor to obtain environment features for data augmentation while mitigating topology imbalance. Additionally, GraphIFE employs a gated mechanism to generate mixed features, enhancing the model’s ability to distinguish invariant node features. Moreover, we proposed two strategies to mitigate the quality inconsistency issue: (1) representation alignment, which align the representation of intra-class nodes, particularly for the minority class; and (2) neighbor label distribution weighting for neighbor sampling, which ensures that the neighbors of synthesized nodes better conform to the distribution of the original dataset. GraphIFE demonstrates its superior performance on the citation network, co-purchasing, and collaboration datasets. For future work, we aim to further optimize GraphIFE to reduce computational overhead while maintaining strong performance. A key limitation is that GraphIFE can encounter out-of-memory (OOM) issues when applied to large-scale graphs, largely due to the high cost of neighbor sampling, which is the most time-consuming stage. Therefore, improving the efficiency of neighbor sampling strategies is an important direction. Moreover, we expect GraphIFE to generalize to other quantity-based heterogeneous information network that exhibit imbalanced node types.

## REFERENCES

- [1] D. J. Cook and L. B. Holder, *Mining graph data*. John Wiley & Sons, 2006.
- [2] W. Ju, Z. Fang, Y. Gu, Z. Liu, Q. Long, Z. Qiao, Y. Qin, J. Shen, F. Sun, Z. Xiao *et al.*, “A comprehensive survey on deep graph representation learning,” *Neural Networks*, p. 106207, 2024.
- [3] S. Wu, F. Sun, W. Zhang, X. Xie, and B. Cui, “Graph neural networks in recommender systems: a survey,” *ACM Computing Surveys*, vol. 55, no. 5, pp. 1–37, 2022.
- [4] L. Yang, Z. Liu, Y. Dou, J. Ma, and P. S. Yu, “Consisrec: Enhancing gnn for social recommendation via consistent neighbor aggregation,” in *International ACM SIGIR Conference On Research And Development in Information Retrieval*, 2021, pp. 2141–2145.
- [5] R. Ying, R. He, K. Chen, P. Eksombatchai, W. L. Hamilton, and J. Leskovec, “Graph convolutional neural networks for web-scale recommender systems,” in *ACM SIGKDD International Conference on Knowledge Discovery and Data Mining*, 2018, pp. 974–983.
- [6] Z. Yang, G. Zhang, J. Wu, J. Yang, S. Xue, A. Beheshti, H. Peng, and Q. Z. Sheng, “Global interpretable graph-level anomaly detection via prototype,” in *ACM SIGKDD Conference on Knowledge Discovery and Data Mining*, 2025, pp. 3586–3597.
- [7] Y. Wei, X. Fu, L. Liu, Q. Sun, H. Peng, and C. Hu, “Prompt-based unifying inference attack on graph neural networks,” in *AAAI Conference on Artificial Intelligence*, vol. 39, no. 12, 2025, pp. 12 836–12 844.
- [8] J. Jumper, R. Evans, A. Pritzel, T. Green, M. Figurnov, O. Ronneberger, K. Tunyasuvunakool, R. Bates, A. Židek, A. Potapenko *et al.*, “Highly accurate protein structure prediction with alphafold,” *nature*, vol. 596, no. 7873, pp. 583–589, 2021.
- [9] X. Wang and M. Zhang, “How powerful are spectral graph neural networks,” in *International Conference on Machine Learning*. PMLR, 2022, pp. 23 341–23 362.
- [10] F. Wu, A. Souza, T. Zhang, C. Fifty, T. Yu, and K. Weinberger, “Simplifying graph convolutional networks,” in *International Conference on Machine Learning*. PMLR, 2019, pp. 6861–6871.
- [11] T. Zhao, X. Zhang, and S. Wang, “GraphSMOTE: Imbalanced node classification on graphs with graph neural networks,” in *ACM International Conference on Web Search and Data Mining*, 2021, pp. 833–841.
- [12] Z. Liu, J. Kang, H. Tong, and Y. Chang, “IMBENS: Ensemble class-imbalanced learning in python,” *arXiv preprint arXiv:2111.12776*, 2023.
- [13] Z. Liu, Y. Li, N. Chen, Q. Wang, B. Hooi, and B. He, “A survey of imbalanced learning on graphs: Problems, techniques, and future directions,” *IEEE Transactions on Knowledge and Data Engineering*, vol. 37, no. 6, pp. 3132–3152, 2025.
- [14] O. Shchur, M. Mumme, A. Bojchevski, and S. Günnemann, “Pitfalls of graph neural network evaluation,” *arXiv preprint arXiv:1811.05868*, 2018.
- [15] L. Galke, I. Vagliano, B. Franke, T. Zielke, M. Hoffmann, and A. Scherp, “Lifelong learning on evolving graphs under the constraints of imbalanced classes and new classes,” *Neural Networks*, vol. 164, pp. 156–176, 2023.
- [16] N. V. Chawla, K. W. Bowyer, L. O. Hall, and W. P. Kegelmeyer, “SMOTE: Synthetic minority over-sampling technique,” *Journal of Artificial Intelligence Research*, vol. 16, pp. 321–357, 2002.
- [17] W.-Z. Li, C.-D. Wang, H. Xiong, and J.-H. Lai, “GraphSHA: Synthesizing harder samples for class-imbalanced node classification,” in *ACM SIGKDD Conference on Knowledge Discovery and Data Mining*, 2023, pp. 1328–1340.
- [18] J. Park, J. Song, and E. Yang, “GraphENS:Neighbor-aware ego network synthesis for class-imbalanced node classification,” in *International Conference on Learning Representations*, 2021.
- [19] Z. Liu, R. Qiu, Z. Zeng, H. Yoo, D. Zhou, Z. Xu, Y. Zhu, K. Welde-meriam, J. He, and H. Tong, “Class-imbalanced graph learning without class rebalancing,” in *International Conference on Machine Learning*, 2024.
- [20] D. Chen, Y. Lin, G. Zhao, X. Ren, P. Li, J. Zhou, and X. Sun, “Topology-imbalance learning for semi-supervised node classification,” *Advances in Neural Information Processing Systems*, vol. 34, pp. 29 885–29 897, 2021.
- [21] Z. Liu, T.-K. Nguyen, and Y. Fang, “Tail-GNN: Tail-node graph neural networks,” in *ACM SIGKDD Conference on Knowledge Discovery & Data Mining*, 2021, pp. 1109–1119.
- [22] J. Song, J. Park, and E. Yang, “TAM: Topology-aware margin loss for class-imbalanced node classification,” in *International Conference on Machine Learning*. PMLR, 2022, pp. 20 369–20 383.
- [23] I. J. Goodfellow, J. Pouget-Abadie, M. Mirza, B. Xu, D. Warde-Farley, S. Ozair, A. Courville, and Y. Bengio, “Generative adversarial nets,” *Advances in Neural Information Processing Systems*, vol. 27, 2014.
- [24] Y. Sui, Q. Wu, J. Wu, Q. Cui, L. Li, J. Zhou, X. Wang, and X. He, “Unleashing the power of graph data augmentation on covariate distribution shift,” *Advances in Neural Information Processing Systems*, vol. 36, 2024.
- [25] P. Sen, G. Namata, M. Bilgic, L. Getoor, B. Galligher, and T. Eliassi-Rad, “Collective classification in network data,” *AI Magazine*, vol. 29, no. 3, pp. 93–93, 2008.
- [26] W. Hamilton, Z. Ying, and J. Leskovec, “Inductive representation learning on large graphs,” *Advances in Neural Information Processing Systems*, vol. 30, 2017.
- [27] T. N. Kipf and M. Welling, “Semi-supervised classification with graph convolutional networks,” in *International Conference on Learning Representations*, 2016.
- [28] P. Veličković, G. Cucurull, A. Casanova, A. Romero, P. Lio, and Y. Bengio, “Graph attention networks,” *International Conference on Learning Representations*, 2017.
- [29] N. Japkowicz and S. Stephen, “The class imbalance problem: a systematic study,” *Intelligent Data Analysis*, vol. 6, no. 5, pp. 429–449, 2002.
- [30] J. M. Johnson and T. M. Khoshgoftaar, “Survey on deep learning with class imbalance,” *Journal of Big Data*, vol. 6, no. 1, 2019.

- [31] L. Qu, H. Zhu, R. Zheng, Y. Shi, and H. Yin, "ImGAGN: Imbalanced network embedding via generative adversarial graph networks," in *ACM SIGKDD Conference on Knowledge Discovery and Data Mining*, 2021, pp. 1390–1398.
- [32] M. Shi, Y. Tang, X. Zhu, D. Wilson, and J. Liu, "Multi-class imbalanced graph convolutional network learning," in *International Joint Conference on Artificial Intelligence*, 2020.
- [33] I. Goodfellow, J. Pouget-Abadie, M. Mirza, B. Xu, D. Warde-Farley, S. Ozair, A. Courville, and Y. Bengio, "Generative adversarial networks," *Communications of the ACM*, vol. 63, no. 11, pp. 139–144, 2020.
- [34] C. Cui, J. Wang, W. Wei, and J. Liang, "Hybrid sampling-based contrastive learning for imbalanced node classification," *International Journal of Machine Learning and Cybernetics*, vol. 14, no. 3, pp. 989–1001, 2023.
- [35] L. Zeng, L. Li, Z. Gao, P. Zhao, and J. Li, "ImGCL: Revisiting graph contrastive learning on imbalanced node classification," in *AAAI Conference on Artificial Intelligence*, 2023, pp. 11 138–11 146.
- [36] D. Yan, G. Wei, C. Yang, S. Zhang *et al.*, "Rethinking semi-supervised imbalanced node classification from bias-variance decomposition," *Advances in Neural Information Processing Systems*, vol. 36, 2024.
- [37] Z. Zhu, H. Xing, and Y. Xu, "Balanced neighbor exploration for semi-supervised node classification on imbalanced graph data," *Information Sciences*, vol. 631, pp. 31–44, 2023.
- [38] J. Liu, Z. Shen, Y. He, X. Zhang, R. Xu, H. Yu, and P. Cui, "Towards out-of-distribution generalization: A survey," *arXiv preprint arXiv:2108.13624*, 2021.
- [39] Y. Mo, X. Wang, S. Fan, and C. Shi, "Graph contrastive invariant learning from the causal perspective," in *AAAI Conference on Artificial Intelligence*, vol. 38, no. 8, 2024, pp. 8904–8912.
- [40] T. Jia, H. Li, C. Yang, T. Tao, and C. Shi, "Graph invariant learning with subgraph co-mixup for out-of-distribution generalization," in *AAAI Conference on Artificial Intelligence*, vol. 38, no. 8, 2024, pp. 8562–8570.
- [41] Y. Liu, X. Ao, F. Feng, Y. Ma, K. Li, T.-S. Chua, and Q. He, "FLOOD: A flexible invariant learning framework for out-of-distribution generalization on graphs," in *ACM SIGKDD Conference on Knowledge Discovery and Data Mining*, 2023, pp. 1548–1558.
- [42] Q. Wang, Y. Wang, Y. Wang, and X. Ying, "Dissecting the failure of invariant learning on graphs," *Advances in Neural Information Processing Systems*, vol. 37, pp. 80 383–80 438, 2024.
- [43] Q. Zhu, N. Ponomareva, J. Han, and B. Perozzi, "Shift-robust gnns: Overcoming the limitations of localized graph training data," *Advances in Neural Information Processing Systems*, vol. 34, pp. 27 965–27 977, 2021.
- [44] Q. Wu, H. Zhang, J. Yan, and D. Wipf, "Handling distribution shifts on graphs: An invariance perspective," *arXiv preprint arXiv:2202.02466*, 2022.
- [45] J. E. Van Engelen and H. H. Hoos, "A survey on semi-supervised learning," *Machine Learning*, vol. 109, no. 2, pp. 373–440, 2020.
- [46] S. Liu, E. Johns, and A. J. Davison, "End-to-end multi-task learning with attention," in *IEEE/CVF Conference on Computer Vision and Pattern Recognition*, 2019, pp. 1871–1880.
- [47] X. Li, Z. Fan, F. Huang, X. Hu, Y. Deng, L. Wang, and X. Zhao, "Graph neural network with curriculum learning for imbalanced node classification," *Neurocomputing*, vol. 574, p. 127229, 2024.
- [48] W. Hu, M. Fey, M. Zitnik, Y. Dong, H. Ren, B. Liu, M. Catasta, and J. Leskovec, "Open graph benchmark: Datasets for machine learning on graphs," in *Advances in Neural Information Processing Systems*, 2020, pp. 22 118–22 133.